JOURNAL OF APPLIED ELECTROCHEMISTRY **26** (1996) 1279–1285

Electrochemical reduction of Fe(II) ions on different solid electrodes in fused $ZnCl_2$–2NaCl mixture

Y. CASTRILLEJO, A. M. MARTINEZ, M. VEGA, P. SANCHEZ BATANERO

Dpto. de Química Analítica, Facultad de Ciencias, Universidad de Valladolid, Prado de la Magdalena s/n, 47005 Valladolid, Spain

Received 5 October 1995; revised 15 April 1996

The electrodeposition of Fe(II) in $ZnCl_2$–2NaCl melt at 450 °C was studied at molybdenum and tungsten electrodes and the results are compared with those obtained at glassy carbon in previous work. The kinetics of the electrodeposition and electrocrystallization of iron were studied, showing that the process is quasireversible, and the values of the kinetic parameters k° and α were obtained. Mass transport towards the electrode is a simple diffusion process and the diffusion coefficient was obtained by applying different electrochemical techniques. Potential step measurements indicate that instantaneous nucleation and growth phenomena play a part in the overall process.

1. Introduction

This study is a part of a systematic research programme focused on the possibility of using mixtures of $ZnCl_2$ with alkali chlorides for the electrolytic reduction of zinc. The effect of impurities in the cell feed and the treatment and recovery of metals, such as iron, contained in ores and industrial zinc wastes can be determined. Development of these processes requires the knowledge of the chemical and electrochemical behaviour of the relevant ions in chloride melts. To reach a better understanding and control of the deposition processes accurate elucidation of the electrochemical deposition mechanism is essential.

Three major factors must be considered when studying cathodic processes: (i) solute mass transport, (ii) electron transfer and (iii) crystal nucleation and growth. Morphologies and structures of deposits as a function of the kinetics and mechanisms of the associated electrode processes offer a fruitful line of development. It is now possible to design and optimize electrolytic processes on a firm electrochemical basis.

The influence of kinetic factors on the electrodeposition processes from molten salts has been discussed by Inman *et al.* [1–3] and others [4, 5]. The importance of nucleation overvoltages/surface phenomena [4, 6, 7], the structure of the electrical double layer and specific effects [3, 8] have also been studied.

Nucleation and growth phenomena in metal deposition depend to a great extent on the substrate on which the electrochemical reduction is performed, not only because of its chemical nature, but also its structural state. The nucleation process is closely related to the active sites existing on the substrate. Thus, with the same bath and the same experimental conditions, different deposits can be obtained using various substrates.

The purpose of this paper is to examine the electrochemical reduction of iron in $ZnCl_2$–2NaCl mixture using various solid substrates such as tungsten and molybdenum as cathodes. The results have been compared with those obtained at glassy carbon electrodes in a previous work [9]. All these materials have different qualities: glassy carbon is amorphous and presents poor interaction with metallic deposits, whilst tungsten and molybdenum are polycrystalline and exhibit better interaction with metallic deposits. We have studied the kinetics of the electron and mass transfer, obtaining the charge-transfer kinetic parameters and the diffusion coefficient of Fe(II) ions. Nucleation and growth phenomena were also investigated.

2. Experimental details

The apparatus and the preparation and purification of the melt have been described previously [9]. The substrates were tungsten and molybdenum wires (1 mm diameter). The electrode active surface area was determined by the depth of immersion and the results were corrected for the height of the meniscus. The counter electrode was a graphite rod or a tungsten wire. The reference electrode consisted of a Pyrex glass tube filled with liquid zinc and molten $ZnCl_2$–2NaCl. A tungsten wire was immersed into the liquid zinc to ensure electrical connection. All the potentials are referred to the Zn(II)/Zn(liq) redox couple.

The addition of Fe(II) to the purified melts was made *in situ* by anodic dissolution of the metal (iron wire 1 mm diameter) at constant current and produced pale yellow solutions at low concentration and dark red–brown solutions at higher concentrations.

Cyclic voltammetry and pulse techniques were performed with a PAR model 273A potentiostat/galvanostat controlled by the M270 software package.

0021-891X

3. Results and discussion

3.1. *Electrochemical window of the $ZnCl_2$–2NaCl mixture with the different cathodic materials*

The electrochemical stability range of the purified $ZnCl_2$–2NaCl melt was examined using voltammetric measurements and was limited cathodically by zinc deposition and anodically by oxidation of chloride ions (Fig. 1). Some authors for other molten chlorides [10, 11] indicated that when using a molybdenum electrode it becomes anodically passivated, a behaviour not observed in the present $ZnCl_2$–2NaCl melt. The ΔE value was calculated from the thermodynamic and experimental data [12] and resulted in a value of 1.715 V. The experimental electroactivity range obtained by extrapolating the limiting anodic polarization curve to zero current is larger than the value calculated above, which indicates an electrochemical reaction overvoltage for the chloride–chlorine system.

3.2. *Electrochemical reduction of Fe (II) ions*

Figure 2 shows some voltammograms for the electroreduction of Fe(II) solutions using different substrates. In all cases, a cathodic peak I_c and a sharp anodic stripping peak I_a were recorded. The shape of the voltammograms, the break corresponding to the beginning of the Fe(II) reduction (characteristic of the formation and reoxidation of a constant activity product) and the peak potential values, all confirm the deposition of Fe(II) and show no evidence for iron solubility. The deposit obtained under potentiostatic conditions was analysed by energy dispersive X-ray

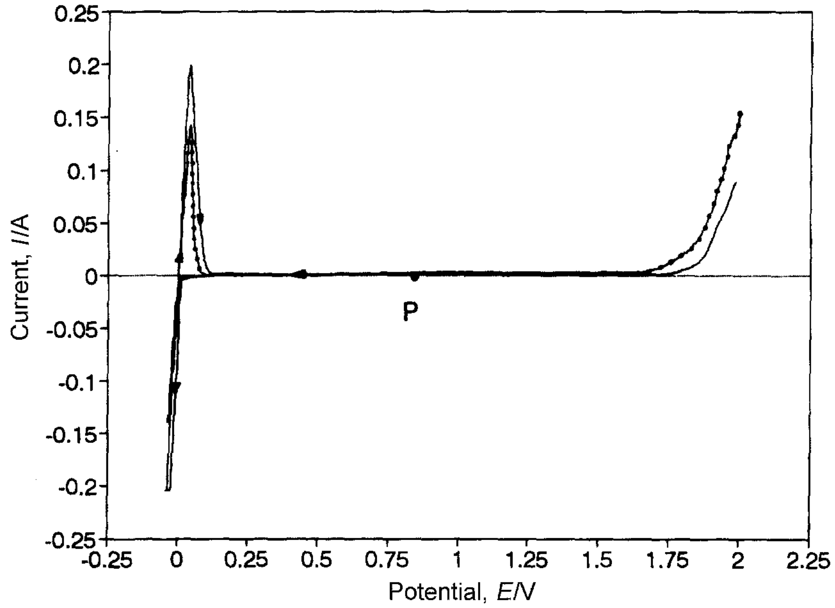

Fig. 1. Cyclic voltammograms obtained at tungsten and molybdenum electrodes on pure $ZnCl_2$–2NaCl melt. Sweep rate 0.2 V s^{-1}. Electrode areas: 0.25 and 0.16 cm^2 for tungsten (————) and molybdenum (-●-●-●-●-), respectively.

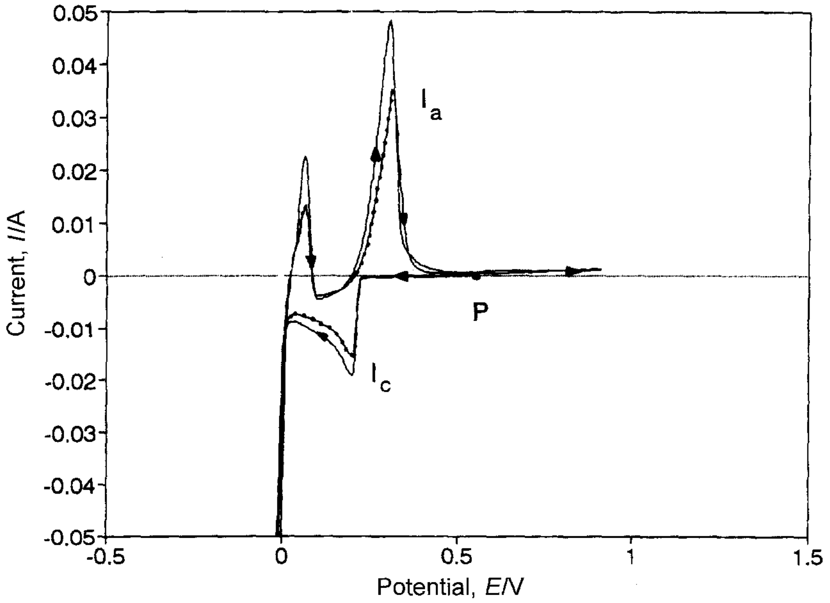

Fig. 2. Typical cyclic voltammogram for the reduction of iron chloride (0.0385 mol kg^{-1}) on a tungsten (————) (0.19 cm^2 electrode area) and molybdenum (-●-●-●-●-) (0.16 cm^2). Sweep rate 0.2 V s^{-1}.

analysis with the scanning microscope (Fig. 3) and by X-ray diffraction, and consisted of pure metallic iron [9].

Cyclic voltammograms for the reduction of iron chloride on a glassy carbon electrode [9] show cathodic peak potential values more negative than those obtained at tungsten and molybdenum substrates. This behaviour may be due to kinetic limitations due to the nucleation phenomena which, especially on glassy carbon substrates, dominate the deposition process.

3.2.1. Reversibility of iron deposition. The voltammetric curves recorded at different potential sweep rates using tungsten and molybdenum as working electrodes (Fig. 4(a) and (b)), show that the cathodic peak potential shifted with increasing sweep rate for values up to about $2.5\,\mathrm{V\,s^{-1}}$ in the former and $0.6\,\mathrm{V\,s^{-1}}$ in the latter (Fig. 4(c)). However, when using glassy carbon as working electrode [9], the cathodic peak potential shifted negatively over the whole sweep rate range. This is probably due to the nonreversibility of the deposition process. Assuming this possibility, the charge-transfer coefficient, α, for iron deposition can be determined by means of the equation [13, 14]:

$$\frac{\Delta E_{\mathrm{p}}}{\Delta \log v} = \frac{2.3\,RT}{2\alpha n F} \qquad (1)$$

The results for the three electrodes are gathered in Table 1.

Further studies of the electrochemical behaviour of iron ion reduction were carried out using chronopotentiometry. Analysis of the variation of the

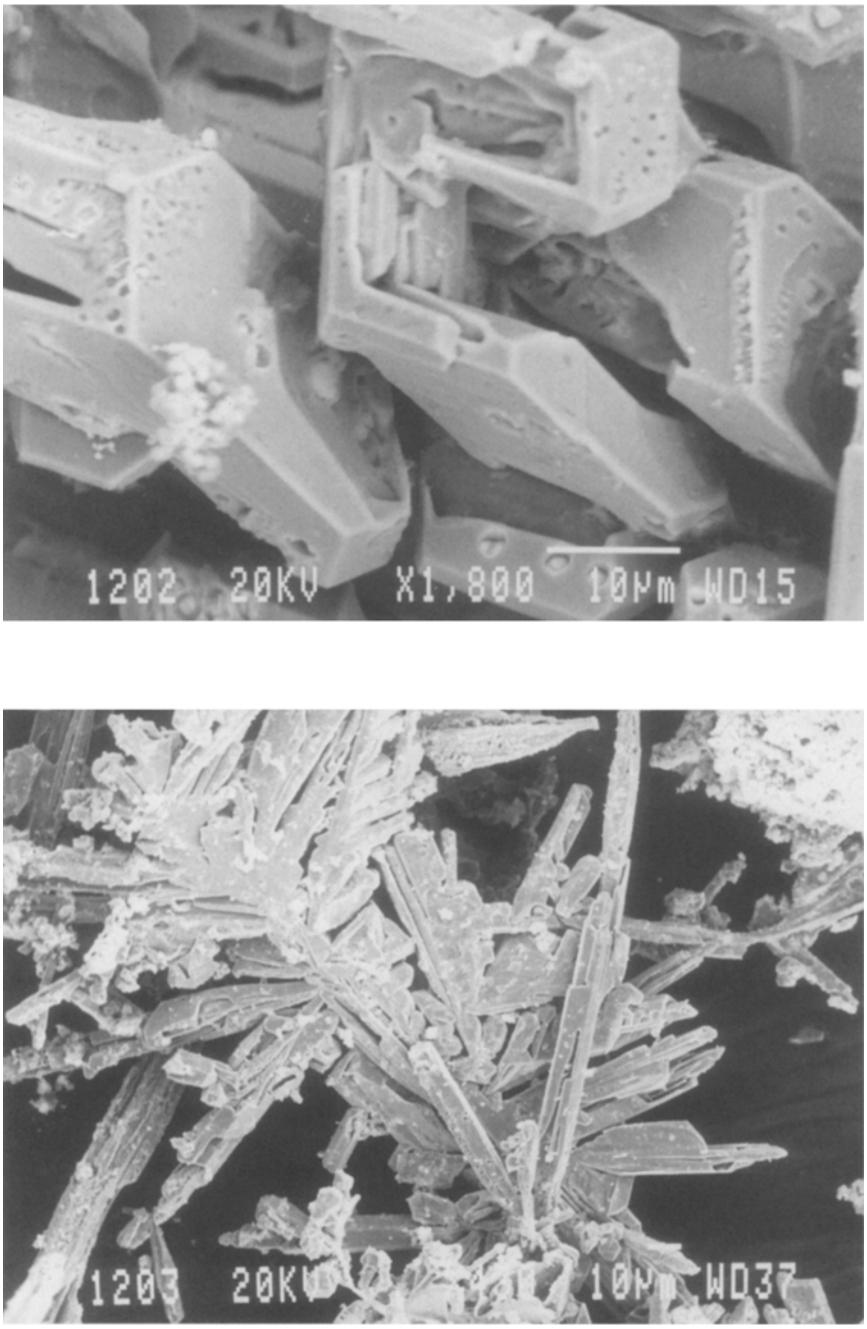

Fig. 3. Micrographs showing iron deposited under different potentiostatic conditions.

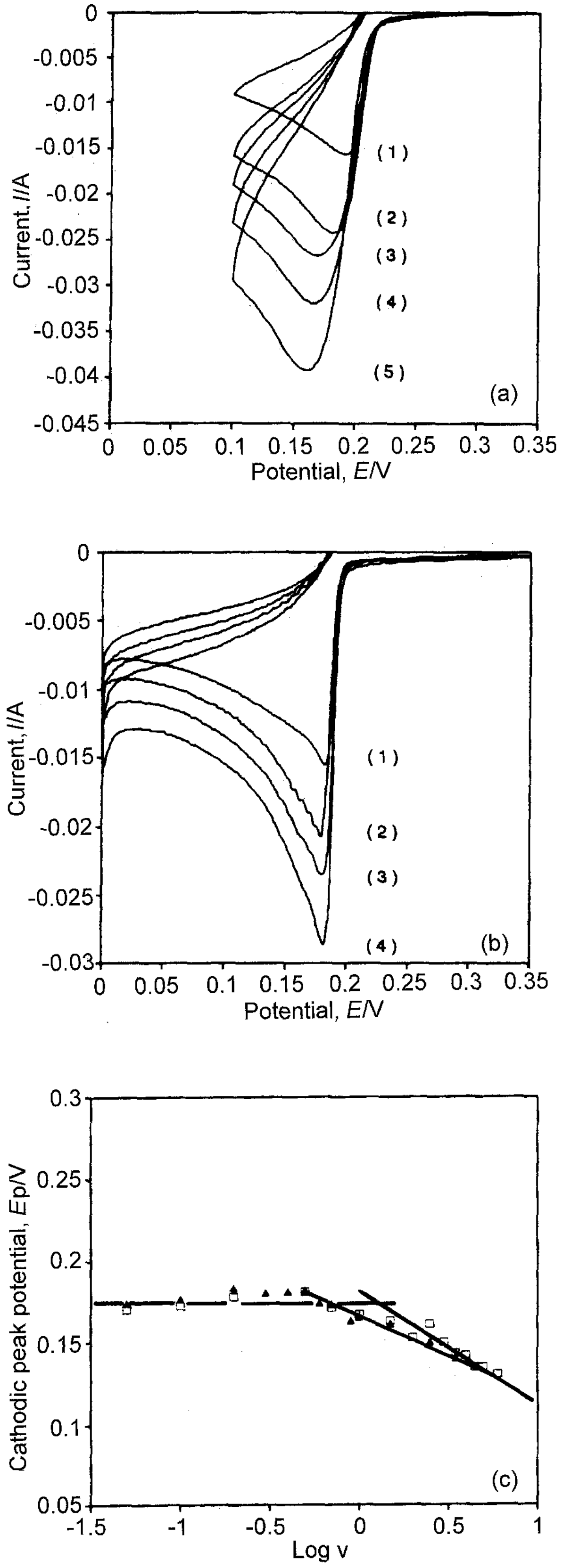

Fig. 4. (a) Voltammetric reduction of iron chloride at a tungsten electrode. Fe(II) concentration of 0.024 mol kg^{-1}. Electrode area 0.31 cm^2. Sweep rates: (1) 0.2; (2) 0.5; (3) 0.7; (4) 1.0; (5) 1.5 V s^{-1}. (b) Voltammetric reduction of iron chloride at a molybdenum electrode. Fe(II) concentration 0.0385 mol kg^{-1}; electrode area 0.19 cm^2; sweep rates: (1) 0.2; (2) 0.3; (3) 0.4; (4) 0.5 V s^{-1}. (c) Variation of the cathodic peak potentials with the logarithm of the sweep rate. (□) tungsten, and (▲) molybdenum substrates.

Table 1. Values of the charge-transfer coefficient, α, for iron deposition obtained by means of the equation $\Delta E_p/\Delta \log \nu = 2.3\,RT/2\alpha nF$ at different substrates

Working electrode	α
Molybdenum	0.41
Tungsten	0.55
Glassy carbon*	0.43

* Value calculated in a previous work [9].

transition time, τ, as a function of the imposed current indicated that the fluxes of Fe(II) species were diffusion controlled (Sand's law). Under these conditions it is possible to perform logarithmic analysis of chronopotentiograms. The electrode potential was found to vary linearly with $\log[1-(t/\tau)^{1/2}]$, but the slopes of the linear part of the curves were different to those expected for a reversible two-electron exchange process.

Convoluted voltammograms were obtained and analysed [15–18]. The curves recorded at different sweep rates were very similar but the direct and reverse scans were not identical (Fig. 5). This behaviour was observed with all the substrates used.

When the convoluted curves were analysed according to a reversible model

$$E = E_{1/2} + \frac{2.3\,RT}{nF}\log\left[\frac{(m^* - m)}{m}\right] \tag{2}$$

plots of the electrode potentials against $\log[(m^* - m)/m^*]$ (where m is the convoluted current and m^* its limiting value) were linear, but the slopes obtained were different from the theoretical value corresponding to a reversible two-electron exchange process indicating that in these conditions the electron transfer rate is significantly lower than that of mass transport.

To confirm these results a logarithmic analysis of the convoluted curves was performed according to a quasireversible model for which the expression corresponding to a process with formation of an insoluble product is [9]:

$$E = E^\circ + \frac{RT}{\alpha nF}\ln k^\circ + \frac{RT}{\alpha nF} \times \ln\left\{\frac{(m^* - m)D^{-1/2} + nFS\exp\left\{\frac{nF}{RT}(E - E^\circ)\right\}}{I}\right\} \tag{3}$$

where k° and α are the charge-transfer rate constant and the transfer coefficient, respectively, and E° the standard potential of the Fe(II)/Fe system [9]. The electrode potential varies linearly with the logarithm of the function M, being:

$$M = \frac{(m^* - m)D^{-1/2} + nFS\exp\left\{\frac{nF}{RT}(E - E^\circ)\right\}}{I} \tag{4}$$

The slope of the linear part of the curve yields the

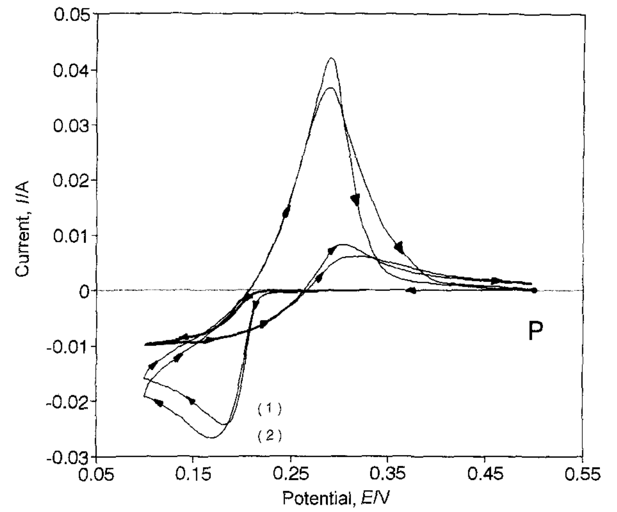

Fig. 5. Several cyclic voltammograms and their corresponding convoluted curves obtained at a tungsten electrode. Sweep rates: (1) $0.5\,V\,s^{-1}$ and (2) $0.7\,V\,s^{-1}$.

Table 2. Values of the charge-transfer kinetic parameters of Fe(II)/Fe(s) exchange obtained by means of the logarithmic analysis of the convoluted voltammograms

Substrate	*$\log k°/\mathrm{cm\,s^{-1}}$*	*α*
Molybdenum	-3.9 ± 0.3	0.45 ± 0.04
Tungsten	-4.4 ± 0.4	0.60 ± 0.05
Glassy carbon*	-4.4 ± 0.5	0.45 ± 0.10

* Value calculated in a previous work [9].

transfer coefficient, α, and from the intercept the charge-transfer rate constant, $k°$, can be calculated. The average values obtained on each substrate are shown in Table 2. From these values, and taking into account the Matsuda and Ayabe criteria [13], the quasireversibility of the iron deposition at all the substrates is verified and it can be deduced that there are no significant differences among the charge transfer rate constant values calculated using the three materials.

3.2.2. Nucleation studies. Voltammograms obtained for iron deposition at glassy carbon, molybdenum and tungsten substrates suggested the presence of nucleation processes. In all cases, and depending on the sweep rate, the cathodic part of the curve shows a cross-over between the cathodic and the anodic going scans (see Fig. 6), which indicates phase formation and growth.

The current transients obtained were particularly sensitive to nucleation and growth phenomena, specially at glassy carbon electrodes [9]; this behaviour has also been observed by Shuzhen *et al.* [19] when studying the electrochemical reduction of Fe(II) ions in the $MgCl_2$–NaCl–KCl eutectic on a tungsten electrode. Figure 7 shows a set of current-transients on molybdenum. These are similar to the transients on glassy carbon, but on molybdenum substrates the current rapidly reaches the limiting value. This increase in current up to a maximum is typical for the formation of a deposit by nucleation and growth of the crystallites. The current decreases while approaching the characteristic response for linear diffusion to a planar electrode (Cottrell condition). Since the rising part of the transient obeyed a $I/t^{1/2}$ dependence, the initial stages at the surface of the substrate of electrochemical deposition of iron can be explained in terms of a model involving instantaneous nucleation.

3.2.3. Fe(II) diffusion. The Sand (Equation 5), Cottrell (Equation 6) and Berzins-Delahay (Equation 7) equations were obeyed. Thus mass transport towards the electrode is a simple diffusional process.

The diffusion coefficients, $D_{Fe(II)}$, given in Table 3 were calculated from chronopotentiometric and chronoamperometric data as well as from the boundary semiintegral values according to the following relations:

$$I\tau^{1/2} = \frac{nFSc_0D^{1/2}\pi^{1/2}}{2} \qquad (5)$$

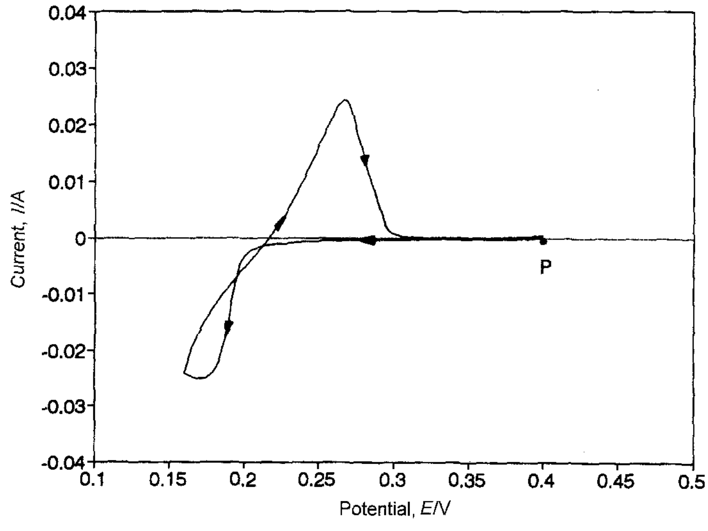

Fig. 6. Cyclic voltammogram illustrating the 'nucleation cross-over effect' on the return sweep for deposition of iron on a tungsten substrate ($0.31\,cm^2$). Fe(II) concentration: $0.024\,mol\,kg^{-1}$; sweep rate: $0.7\,V\,s^{-1}$.

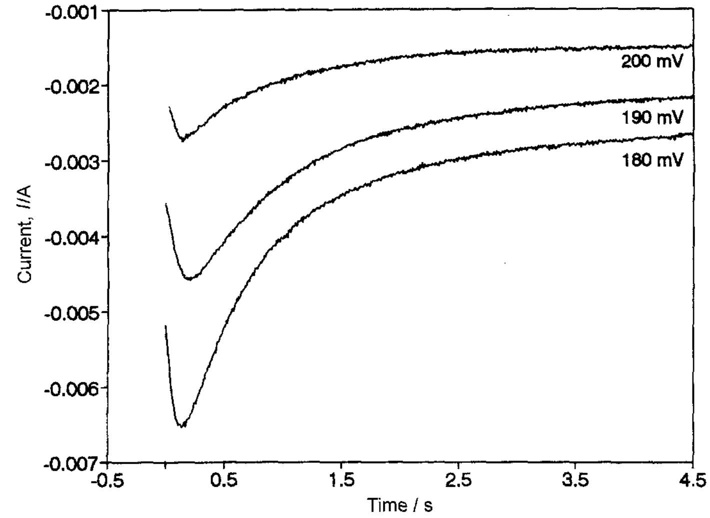

Fig. 7. Potentiostatic current transients for electrochemical deposition of iron on a molybdenum electrode in $ZnCl_2$–2NaCl at 450 °C. Fe(II) concentration: 0.026 mol kg^{-1}; electrode area: 0.22 cm^2. The applied potentials are indicated on the curves.

$$I = nFSc_0D^{1/2}(\pi t)^{-1/2} \tag{6}$$

$$m^* = nFSc_0D^{1/2} \tag{7}$$

where c_0 is the bulk concentration of the electroactive species, D its diffusion coefficient and S the electrode surface area. The differences between the calculated values are mainly related to the difficulty in determining the exact active electrode areas.

In the case of a quasireversible process, most authors consider that the Berzins–Delahay equation:

$$I_\mathrm{P} = 0.610\, nFSc_0\left(\frac{nF}{RT}\right)^{1/2} v^{1/2}D^{1/2} \tag{8}$$

for a reversible diffusion-controlled process can be used. Taking into account the confidence levels achieved, the diffusion coefficients calculated from the slope of the I_p against $v^{1/2}$ plot were of the same order of magnitude as those obtained by other electrochemical techniques. This indicates that in the present conditions it is correct to apply this equation despite the non-reversibility of the electroreduction process.

4. Conclusions

Using voltammetric, chronopotentiometric, chronoamperometric and convolution techniques it was possible to determine the mass and the charge transfer kinetics occurring in the electrochemical reduction and oxidation of Fe(II) ions on tungsten, molybdenum and glassy carbon substrates.

Table 3. Iron (II) diffusion coefficients ($10^5 D/cm^2\,s^{-1}$) obtained on each substrate by different electrochemical techniques

Technique	*Glassy carbon*	*Mo*	*W*
Convolution	1.2 ± 0.4	1.3 ± 0.2	1.0 ± 0.1
Chronopotentiometry	1.2 ± 0.3	1.2 ± 0.1	1.5 ± 0.2
Chronoamperometry	1.6 ± 0.4	1.1 ± 0.1	0.9 ± 0.1
Voltammetry	0.9 ± 0.1	0.8 ± 0.1	0.9 ± 0.1

The Fe(II)/Fe(0) exchange was found to be quasireversible at all substrates used and the cathodic process depends strongly on the sweep rate. The results obtained showed that the mass-transport is diffusion controlled. The intrinsic rate constant $k°$ and the transfer coefficient α of the Fe(II)/Fe(0) system were also obtained from logarithmic analysis of the convoluted curves by applying the equation for a soluble–insoluble quasireversible process.

Potential step measurements indicate that instantaneous nucleation and growth phenomena play a part in the overall process at all the substrates studied. Thus, depending on the controlled electrochemical parameters, different iron deposits can be obtained.

Acknowledgements

Authors are grateful to D.G.I.C.Y.T. CE93-0017 and Junta de Castilla y León, C. de Cultura y Turismo (Spain) for financial support of this research. Also, A.M.M. wishes to thank D.G.I.C.Y.T. for a doctoral grant.

References

[1] D. Inman and S. H. White, International Symposium 'Molten Salt Electrolysis in Metal Production', Grenoble, IMM (1977) p. 51.
[2] D. Inman, R. S. Sethi and R. Spencer, *J. Electroanal. Chem.* **29** (1971) 137.
[3] A. D. Graves and D. Inman, *in* 'Electromotive Force Measurements in High Temperature Systems' (edited by C. B. Alcock), IMM, London (1968) p. 187.
[4] S. Senderoff, *Metall. Rev.* **11** (1966) 97.
[5] S. M. Selis, *J. Phys. Chem.* **72** (1968) 1442.
[6] G. J. Hills, D. J. Schiffrin and J. Thompson, *Electrochim. Acta* **19** (1974) 657.
[7] C. Decroly, C. Mukhtar and R. Winand, *J. Electrochem. Soc.* **115** (1968) 905.
[8] A. D. Graves and D. Inman, *J. Electroanal Chem.* **25** (1970) 357.
[9] Y. Castrillejo, A. M. Martínez, M. Vega, E. Barrado and G. Picard, *ibid.* **397** (1995) 139.
[10] A. K. Vijh, *Corros. Sci.* (1971) 161.

[11] J. C. Gabriel, J. Bouteillon, J. C. Poignet and J. M. Roman, *J. Electrochem. Soc.* **141** (9) (1994) 2286.

[12] I. Barin and O. Knacke, 'Thermochemical Properties of Inorganic Substances', Springer-Verlag, Berlin (1973) p. 876.

[13] A. J. Bard and L. R. Faulkner, 'Electrochemical Methods: Fundamentals and Applications', Wiley, New York (1980).

[14] D. D. McDonald, 'Transient Techniques in Electrochemistry', Plenum Press, New York (1977).

[15] J. C. Imbeaux and J. M. Saveant, *J. Electroanal. Chem.* **44** (1973) 169.

[16] J. M. Saveant and D. Tessier, *ibid.* **61** (1975) 251.

[17] *Idem, ibid.* **65** (1975) 57.

[18] K. B. Oldhman, *Anal. Chem.* **44** (1972) 196.

[19] D. Shuzhen, P. Dudley and D. Inman, *J. Electroanal. Chem.* **142** (1982) 215.